

Supporting Information

Multicolored Fluorescence Variation of a New Carbazole-Based AIEE Molecule by External Stimuli

Yan Liu,^{ae} Aisen Li,^{bc} Zhimin Ma,^c Weiqing Xu,^b Zhiyong Ma,^{*a} and Xinru Jia^d

^a Beijing State Key Laboratory of Organic-Inorganic Composites, College of Chemical Engineering, Beijing University of Chemical Technology, Beijing 100029, China. E-mail: mazhy@mail.buct.edu.cn

^b State Key Laboratory for Supramolecular Structure and Materials, Institute of Theoretical Chemistry, College of Physics, Jilin University, Changchun 130012, China.

^c National high-tech industrial development zone in Jingdezhen, Jingdezhen, 333000, China.

^d Beijing National Laboratory for Molecular Sciences, Key Laboratory of Polymer Chemistry and Physics of the Ministry of Education, College of Chemistry and Molecular Engineering, Peking University, Beijing 100871, China.

^e These authors contributed equally.

1. Materials and General Methods

All the solvents and reactants were purchased from commercialized companies and used as received without further purification except for specifying otherwise.

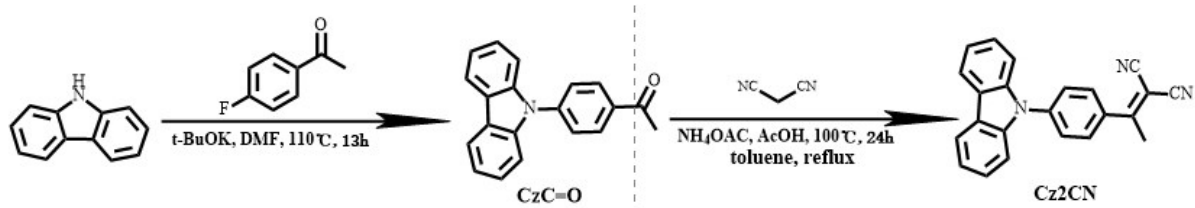
^1H NMR was recorded on the 400 MHz (Bruker ARX400) and ^{13}C NMR spectra were recorded on the Bruker 125 MHz spectrometer at room temperature with CDCl_3 as the solvent and tetramethylsilane (TMS) as the internal standard. ESI high resolution mass-spectra (HRMS) were acquired on a Bruker Apex IV FTMS mass spectrometer. UV-Vis spectra were acquired on the Hitachi U-4100 UV-vis spectrophotometer. Steady fluorescence spectra were performed on the Hitachi F-7000 or Edinburgh Instruments FLS920 fluorescence spectrophotometer. The calculation of quantum yield was performed on the Nanolog/FluoroLog-3-2-Ihr320/Edinburgh Instruments FLS980 fluorescence spectrophotometer combined measurement system for infrared fluorescence equipped with an integrating sphere. Fluorescence lifetime were acquired on the Lifespec-Red Picosecond Lifetime Spectrometer/Edinburgh Instruments FLS980 fluorescence spectrophotometer ($\lambda_{\text{ex}}=365\text{nm}$). The particle size distribution (dynamic light scattering) was measured on a wide-angle static dynamic synchronous laser scattering instrument LV/CGS-3. Differential scanning calorimetry (DSC) measurement was carried out by using TA instruments Q100 DSC. Wide angle X-rays diffraction (WAXD) experiments were measured on a Philips X'PertPro diffractometer with a 3 kW ceramic tube as the X-ray source ($\text{Cu K}\alpha$) and an X'celerator detector.

Single crystal X-ray diffraction data were collected with a NONIUS KappaCCD diffractometer with graphite monochromator and $\text{Mo K}\alpha$ radiation [$\lambda (\text{MoK}\alpha) = 0.71073 \text{ \AA}$]. Structures were solved by direct methods with SHELXS-97 and refined against F2 with SHELXS-97.

Hydrostatic pressure experiments were carried out by using diamond anvil cell (DAC) equipment with silicon oil as pressure-transmitting medium. High pressure experiments were

performed using symmetric diamond anvil cells (DACs) at room temperature. The culet diameter of the diamond anvils was 500 μm . The crystal was placed in the holes (diameter: ca. 170 μm) of a T301 steel gasket, which was pre-indented to a thickness of 50 μm . The silicon oil was used as pressure transmitting medium (PTM). A small ruby chip was inserted into the sample compartment for in situ pressure calibration according to the R1 ruby fluorescence method. The photoluminescence measurements under high pressure were performed on a QE65000 Scientific-grade spectrometer in the reflection mode. The 365 nm line of a laser with a power of 10 mW was used as the excitation source. The images of the powder under 355 nm line of a laser with a power of 10 mW were taken by putting the DAC containing the sample on a Nikon fluorescence microscope. All experiments were carried out at room temperature.

2. Synthesis of targeted molecule Cz2CN



Scheme S1. The synthetic route to Cz2CN.

Compound CzC=O was synthesized according to literature report. ¹

Cz2CN

CzC=O (570.7 mg, 2.0 mmol), malonitrile (145.3 mg, 2.2 mmol), Ammonium acetate (169.6 mg, 2.2 mmol), acetic acid (0.33 mL, 6 mmol) were added to a 100 mL round-bottomed flask containing 20 mL of toluene. The mixed solution was refluxed at $100\text{ }^\circ\text{C}$ for 24h. After the reaction was over, the resultant mixture was cooled down to room temperature and the solvent was removed under reduced pressure. The crude product was purified by column chromatography using dichloromethane and petroleum ether (v/v, 1:4) as the eluent to obtain 493.4 mg pure product as light yellow powder. Yield: 74%.

^1H NMR (400 MHz, CDCl_3) δ /ppm: 8.16 (d, $J = 1.1\text{ Hz}$, 1H), 8.14 (t, $J = 1.0\text{ Hz}$, 1H), 7.86 – 7.82 (m, 2H), 7.79 – 7.75 (m, 2H), 7.51 (dt, $J = 8.2, 1.0\text{ Hz}$, 2H), 7.44 (ddd, $J = 8.2, 7.0, 1.3\text{ Hz}$, 2H), 7.34 (td, $J = 7.4, 7.0, 1.1\text{ Hz}$, 2H), 2.75 (s, 3H).

^{13}C NMR (101 MHz, CDCl_3) δ /ppm: 141.70, 140.05, 133.97, 129.35, 126.91, 126.33, 123.97, 120.89, 120.55, 112.92, 112.74, 109.72, 24.23.

HR-ESI-MS Calcd. For $\text{C}_{23}\text{H}_{16}\text{N}_3$ $[\text{M}+\text{H}]^+$: 334.134086. Found: 334.133874.

3. NMR spectra and HR-MS of Cz2CN

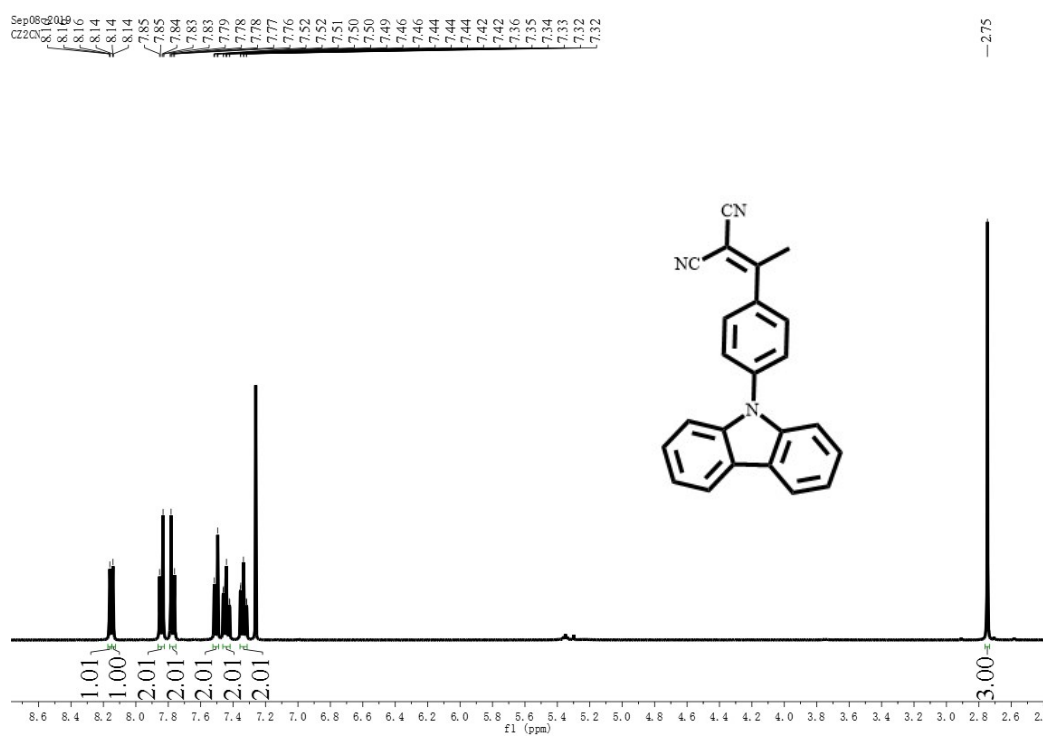


Figure S1. ¹H NMR spectra of Cz2CN.

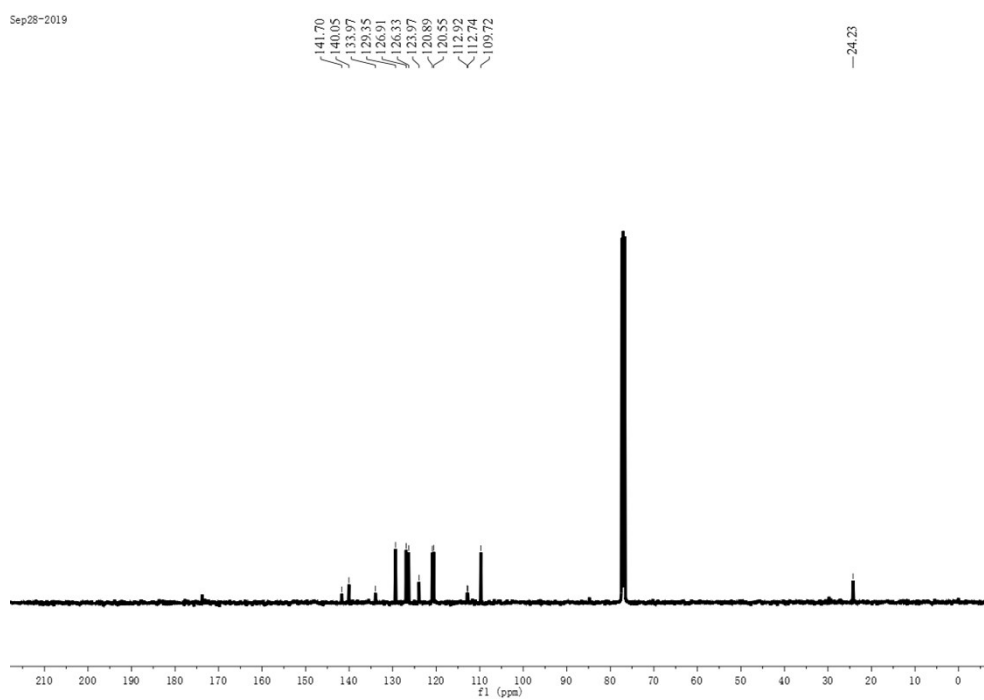


Figure S2. ¹³C NMR spectra of Cz2CN.

Peking University Mass Spectrometry Sample Analysis Report

Analysis Info

Analysis Name	FTMS-19100117_Pos_20191016_000001.d	Acquisition Date	10/16/2019 8:37:54 AM
Sample	CZ2CN	Instrument	Bruker Solarix XR FTMS
Comment		Operator	Peking University

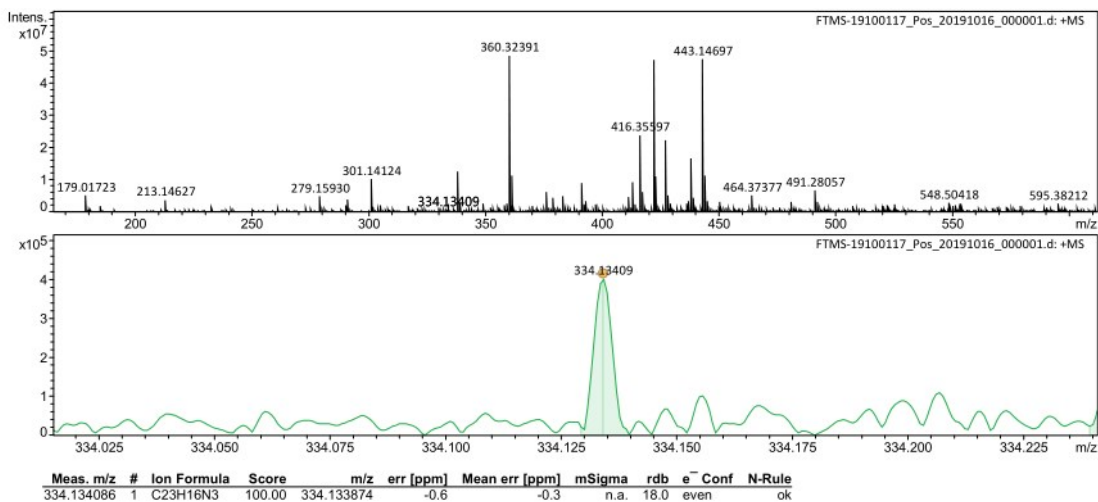


Figure S3. HR-MS spectra of Cz2CN.

4. Detailed data of Cz2CN single crystal

Table S1. Data table of Cz2CN single crystal.

Identification code	Cz2CN
CCDC Number	1988014
Empirical formula	C ₂₃ H ₁₅ N ₃
Formula weight	333.38
Temperature	283(2) K
Wavelength	0.71073 Å
Crystal system	monoclinic
Space group	<i>P</i> 1 21/ <i>c</i> 1
Unit cell dimensions	a = 8.4001(4) Å, α = 90.00°. b = 27.6987(14) Å, β = 99.621(2)°. c = 7.4900(4) Å, γ = 90.00°.
Volume	1718.20(15) Å ³
Z	4
Density (calculated)	1.289 Mg/m ³

Absorption coefficient	0.077 mm ⁻¹
F(000)	696
Theta range for data collection	2.942 to 27.529°.
Index ranges	-10<=h<=9, -35<=k<=35, -9<=l<=9
Reflections collected	27768
Independent reflections	3947 [R(int) = 0.0543]
Final R indices [I>2sigma(I)]	R1 = 0.0500, wR2 = 0.1240
R indices (all data)	R1 = 0.0851, wR2 = 0.1580

5. The AIEE property of Cz2CN

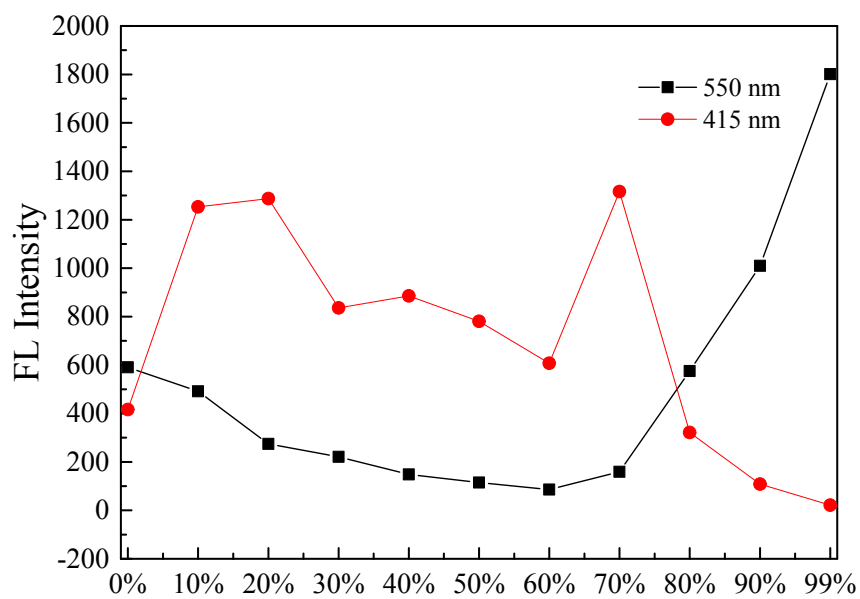


Figure S4. The fraction of water with fluorescence intensity change of Cz2CN (20 μM) in THF/water mixtures plot($\lambda_{ex}=365$ nm) .



Figure S5. Fluorescence life time decay profiles of **Cz2CN** (20 μM) in mixed solvents of THF/water with water fraction (f_w) is 99%.

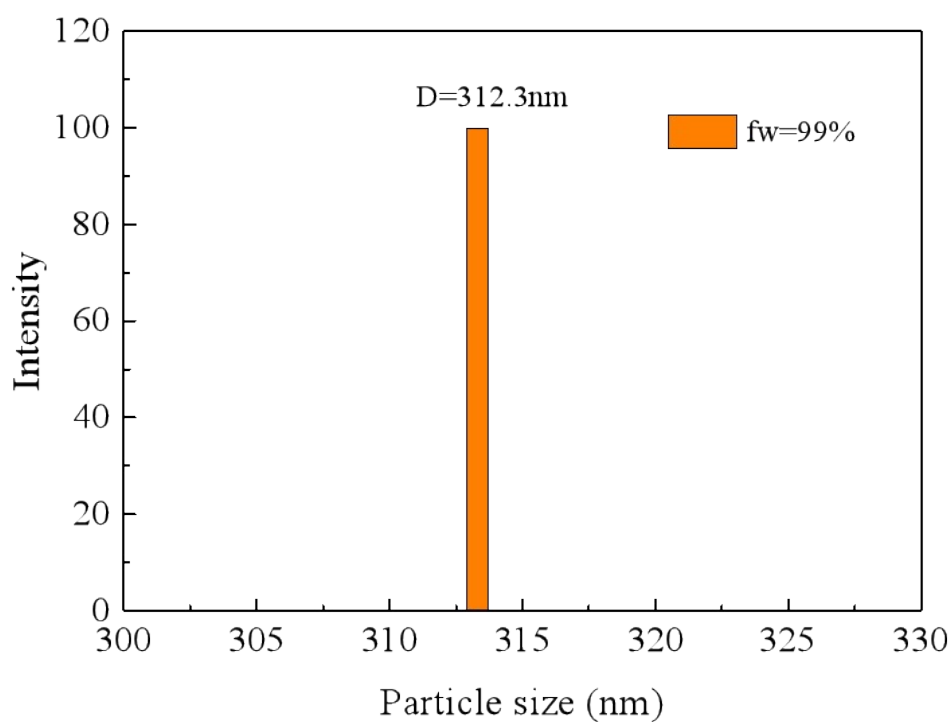


Figure S6. The particle diameter distributions of the **Cz2CN** in THF/water mixtures with 99% water content.

Table S2. Change of Fluorescence Parameters against f_w .

sample(f_w)	λ_{em} (nm)	QY(%)	τ (ns)	$kr(10^6 \text{ S}^{-1})$	$knr(10^6 \text{ S}^{-1})$
0%	550	1.76	4.84	3.64	202.97
99%	550	0.77	1.71	1.025	107.04

$\lambda_{ex}=365$ nm.

6. HOMO and LUMO

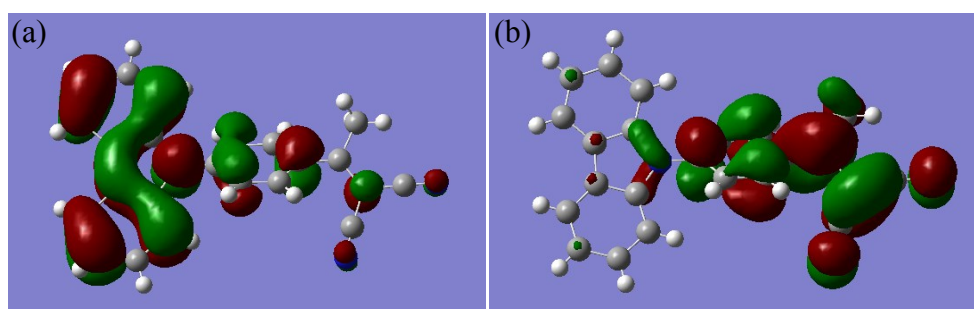


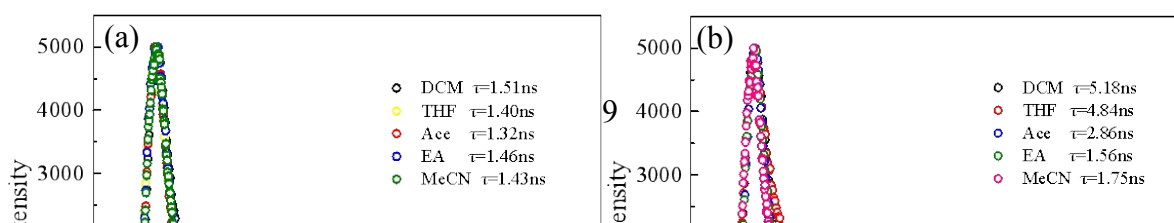
Figure S7. Optimized geometry and calculated spatial electron distributions of HOMO (a); and LUMO (b) of Cz2CN.

7. The solvatochromic property of Cz2CN

Table S3. Photophysical properties of Cz2CN in different solvents.

solvent	Δf	$\lambda_{abs.}(nm)$	$\lambda_{em.}(nm)$		$\Delta V(cm^{-1})$	$\Phi_{F-total}(\%)$	$\Phi_{F-LE}(\%)$	$\Phi_{F-ICT}(\%)$
			LE	ICT				
Hexane	0.0012	379	427	483	5681.3	14.37	12.19	2.18
Toluene	0.012	383	434	497	5988.9	13.09	10.63	2.46
Tetrahydrofuran	0.210	371	434	539	8134.0	10.02	8.26	1.76
Dichloromethane	0.219	380	435	550	8401.3	11.99	4.96	7.03
Acetone	0.284	365	434	560	9540.1	12.61	8.79	3.82
Ethanol	0.288	371	436	550	8772.4	6.99	3.61	3.38
Acetonitrile	0.305	364	432	560	9615.4	8.78	4.52	4.26

$\lambda_{ex}=365$ nm.



@415nm

@~550nm

Figure S8. Fluorescence life time decay profiles of **Cz2CN** (20 μ M) in different organic solvent (a) $\lambda_{em}=415$ nm and (b) $\lambda_{em}\approx 550$ nm.

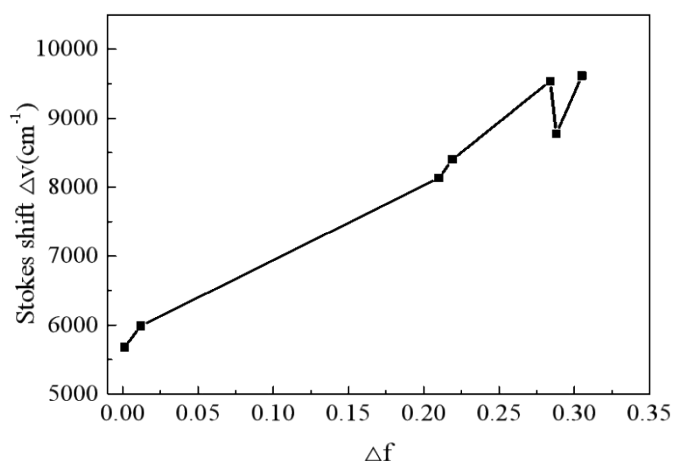


Figure S9. Stokes shift (Δv) of **Cz2CN** as a function of the solvent polarity parameter (Δf).

$$\Delta f = \frac{\varepsilon - 1}{2\varepsilon + 1} - \frac{n^2 - 1}{2n^2 + 1} \quad (\text{eq. 1})$$

$$\Delta v = v_a - v_e = \frac{2(\mu_e - \mu_g)^2}{hca^3} \Delta f + \text{constant} \quad (\text{eq. 2})$$

In which Δv stands for the Stokes shift, v_a and v_e represent the maximum absorption and emission wavenumbers (cm^{-1}), respectively. The letter h is Planck's constant, c is the speed of light in vacuum, a is the Onsager radius. μ_e and μ_g are the permanent dipole moments of the excited state and the ground state, respectively. The letter ε is the static dielectric constant of the solvent, n is the refractive index, and Δf is the orientation polarizability.²

8. Detailed data of Cz2CN single crystal

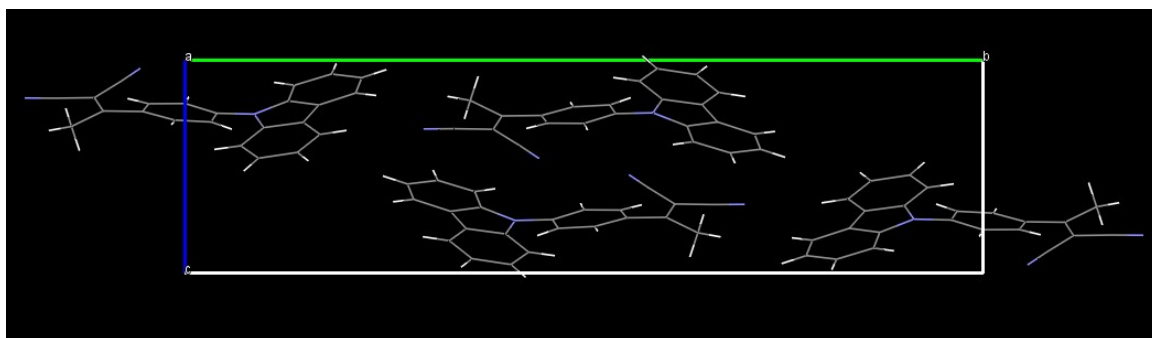


Figure S10. The single crystal unit of **Cz2CN** viewing along a axis.

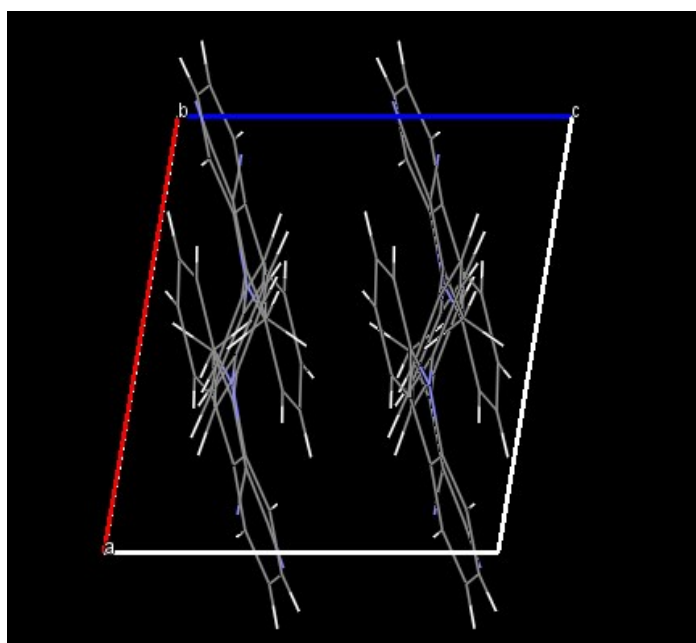


Figure S11. The single crystal unit of **Cz2CN** viewing along b axis.

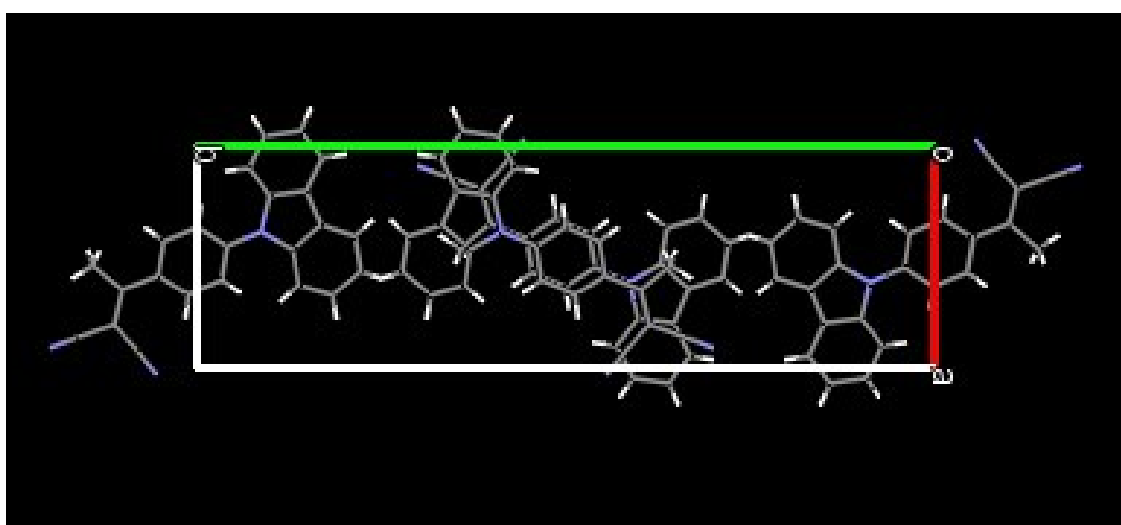


Figure S12. The single crystal unit of **Cz2CN** viewing along c axis.

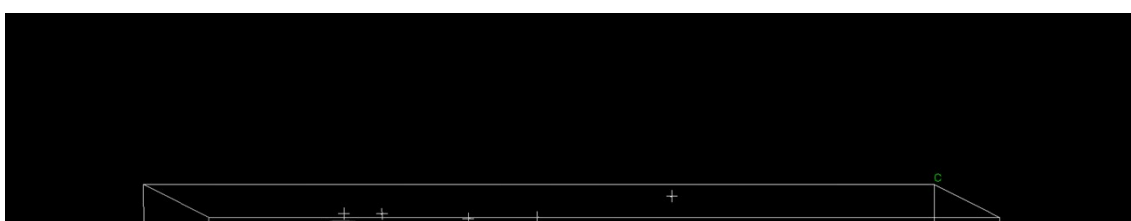


Figure S13. The centroid distance in the molecular packing of **Cz2CN**.

9. Fluorescence decay profiles of **Cz2CN**

Table S4. Data table of **Cz2CN** initial powder and ground powder.

sample	λ_{em} (nm)	QY(%)	τ (ns)	$k_r(10^6 \text{ S}^{-1})$	$k_{nr}(10^6 \text{ S}^{-1})$
initial powder	474	40.4	7.01	57.63	82.37
ground powder	520	21.4	3.53	60.62	219.38

$\lambda_{ex}=365 \text{ nm}$; Radiative decay rate $k_r=\phi/\tau$; Nonradiative decay rate $k_{nr}=1/\tau-k_r$.

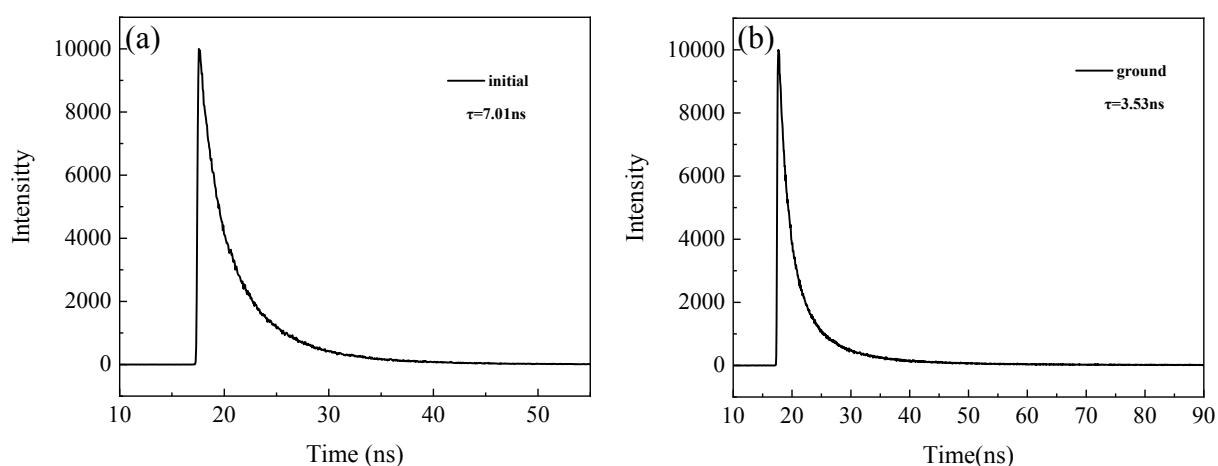


Figure S14. Fluorescence life time decay profiles of **Cz2CN** in (a) the initial powder and (b) the ground powder.

10. XRD curves of **Cz2CN**

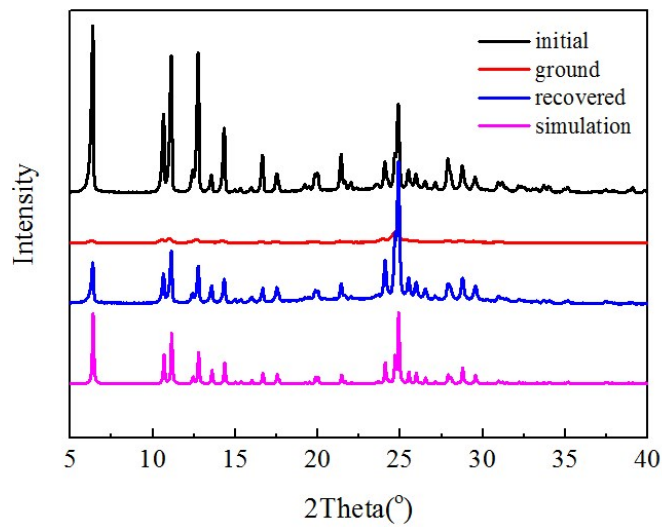


Figure S15. XRD curves of the original powder, the ground powder, the recovered powder and the simulated result.

11. DSC curves of the original powder and ground powder

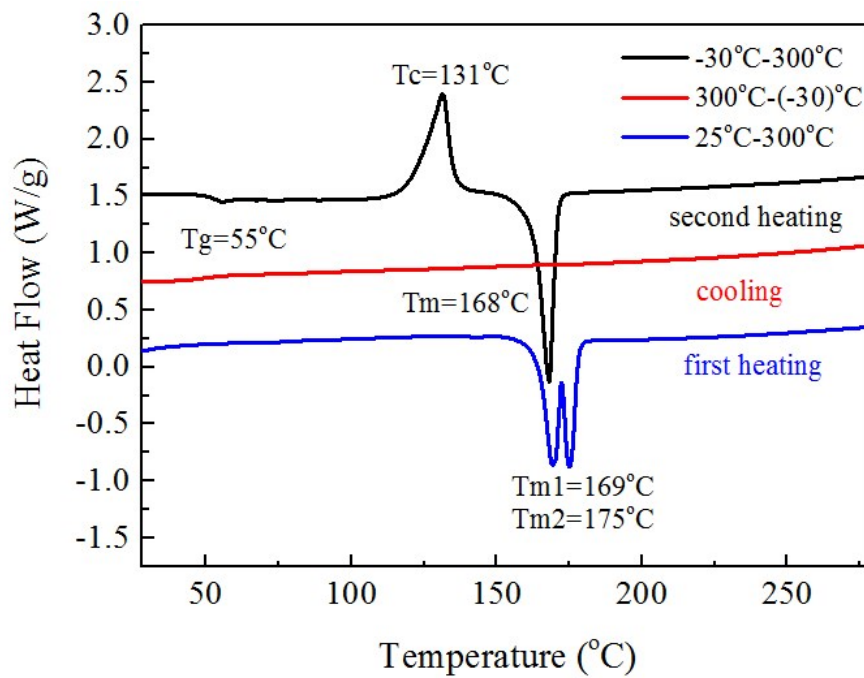


Figure S16. DSC curves of the original powder.

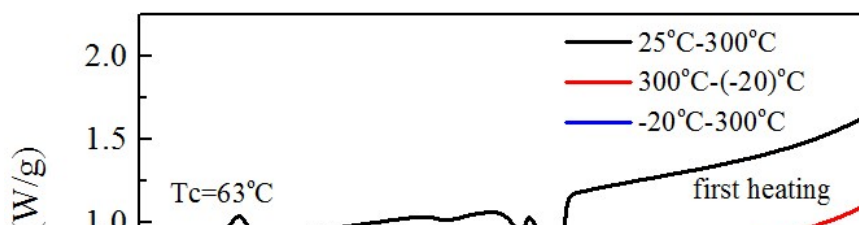


Figure S17. DSC curves of the ground powder.

12. Reversibility between compression and decompression

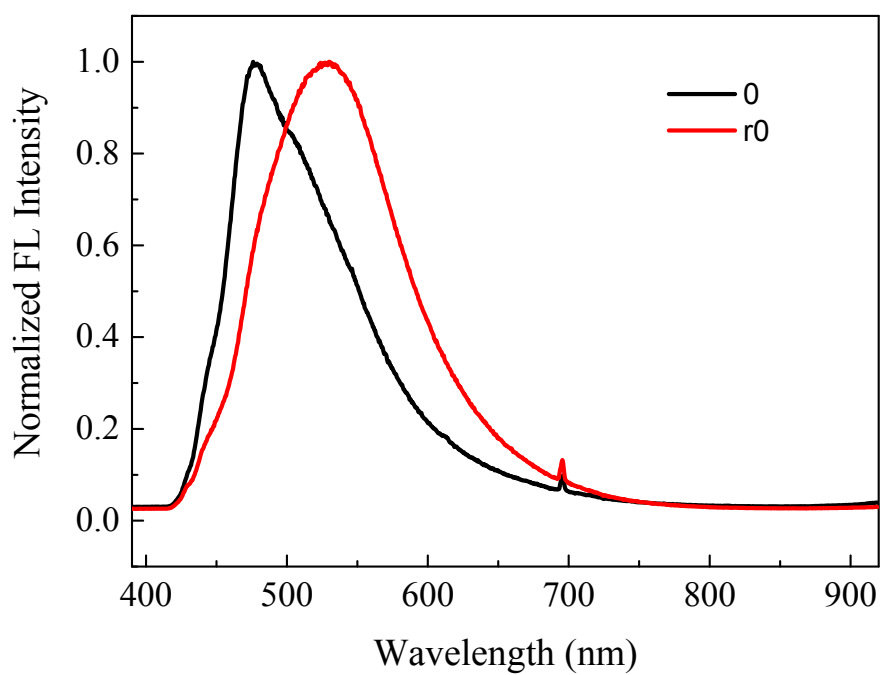


Figure S18. Fluorescent spectra of Cz₂CN single crystal at 0 GPa (before compression and after release) .

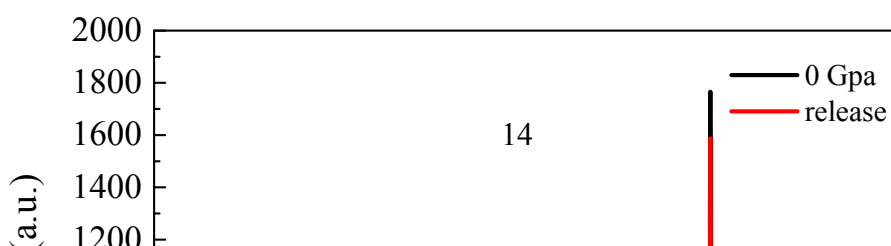


Figure S19. Raman spectra of **Cz2CN** single crystal at 0 GPa (before compression and after release) .

References

- [1] R. R. Zhong, Q. Yin, H. P. Ling, Q. Chen, W. H. Luo and B. H. Han, *polymer*, 2018, **143**, 87-95.
- [2] Z. M. Wang, Y. Feng, S. T. Zhang, Y. Gao, Z. Gao, Y. M. Chen, X. J. Zhang, P. Lu, B. Yang, P. Chen, Y. G. Ma and S. Y. Liu, *PCCP*, 2014, **16**, 20772.